

Ocean Ambient Noise Studies for Shallow and Deep Water Environments

Martin Siderius and Lanfranco Muzi
Portland State University
Electrical and Computer Engineering Department
1900 SW 4th Ave., Portland, OR 97201
Phone:(503) 725-3223 fax:(503) 725-3807 Email: siderius@pdx.edu

Award Number: N00014-12-1-0017

<http://www.ece.pdx.edu/Faculty/Siderius.php>

LONG-TERM GOALS

The objective of this research is to study the ocean ambient noise field by means of new physics-based processing techniques, to determine ways to exploit noise for environmental characterization and to improve sonar-system performance.

OBJECTIVES

Effective performance prediction of active and passive sonar systems relies on accurate modeling of sound propagation in the environment of the target and receiver. In shallow littoral water, propagation is affected by interaction with the acoustic waveguide boundaries, *i.e.* the sea surface and the seabed. The seabed reflection loss in particular is a primary contribution to the transmission loss, and is included in shallow-water propagation models as a power reflection loss coefficient, a function of frequency and grazing angle.

A simple passive technique for estimating the bottom loss by beamforming the ambient-noise field using a vertical line array has been developed by Harrison and Simons [Harrison, 2002]. The advantages of passive bottom-survey techniques include simpler measurement requirements, decreased risk of counter-detection, and minimal environmental impact. However, beamforming has some inherent limitations, which affect in particular the angular resolution: All other array parameters being equal, the angular resolution improves when the array length increases. With increasing interest for short arrays, which can be more easily deployed (even on autonomous underwater vehicles) and potentially eliminate array-mismatch errors due to geometric deformation of the array, poor angular resolution becomes a matter of concern. In recent work, we have proposed a physics-based processing technique for improving the angular resolution

Report Documentation Page				Form Approved OMB No. 0704-0188	
Public reporting burden for the collection of information is estimated to average 1 hour per response, including the time for reviewing instructions, searching existing data sources, gathering and maintaining the data needed, and completing and reviewing the collection of information. Send comments regarding this burden estimate or any other aspect of this collection of information, including suggestions for reducing this burden, to Washington Headquarters Services, Directorate for Information Operations and Reports, 1215 Jefferson Davis Highway, Suite 1204, Arlington VA 22202-4302. Respondents should be aware that notwithstanding any other provision of law, no person shall be subject to a penalty for failing to comply with a collection of information if it does not display a currently valid OMB control number.					
1. REPORT DATE 30 SEP 2013		2. REPORT TYPE		3. DATES COVERED 00-00-2013 to 00-00-2013	
4. TITLE AND SUBTITLE Ocean Ambient Noise Studies for Shallow and Deep Water Environments				5a. CONTRACT NUMBER	
				5b. GRANT NUMBER	
				5c. PROGRAM ELEMENT NUMBER	
6. AUTHOR(S)				5d. PROJECT NUMBER	
				5e. TASK NUMBER	
				5f. WORK UNIT NUMBER	
7. PERFORMING ORGANIZATION NAME(S) AND ADDRESS(ES) Portland State University, Department of Electrical and Computer Engineering, 1900 SW Fourth Avenue, Portland, OR, 97207				8. PERFORMING ORGANIZATION REPORT NUMBER	
9. SPONSORING/MONITORING AGENCY NAME(S) AND ADDRESS(ES)				10. SPONSOR/MONITOR'S ACRONYM(S)	
				11. SPONSOR/MONITOR'S REPORT NUMBER(S)	
12. DISTRIBUTION/AVAILABILITY STATEMENT Approved for public release; distribution unlimited					
13. SUPPLEMENTARY NOTES					
14. ABSTRACT					
15. SUBJECT TERMS					
16. SECURITY CLASSIFICATION OF:			17. LIMITATION OF ABSTRACT Same as Report (SAR)	18. NUMBER OF PAGES 10	19a. NAME OF RESPONSIBLE PERSON
a. REPORT unclassified	b. ABSTRACT unclassified	c. THIS PAGE unclassified			

of short arrays and investigated its application to measured data as well as its limitations [Publications #1 and #2].

APPROACH

The research has included the development of a new derivation in frequency-wavenumber domain of the power reflection coefficient from the array spatial coherence function (providing further theoretical support for Harrison and Simons' technique, whose original justification was based on an energy-flux argument), and the development of the *synthetic-array processor*, a processing technique that exploits the physical properties of the noise field to improve the angular resolution of the array. The new derivation reveals the dependence on array location and provides factors for providing corrections for refraction and volume absorption.

BOTTOM-LOSS ESTIMATION THROUGH BEAMFORMING OF AMBIENT NOISE

For a wave front of frequency ω incident upon the bottom at grazing angle $\theta_b > 0$ (see Figure 1 for the definition of all geometric quantities), the bottom loss is defined as:

$$BL(\theta_b, \omega) = -10 \text{Log} R(\theta_b, \omega), \quad (1)$$

where $R(\theta_b, \omega)$ is the plane-wave power reflection coefficient of the bottom. Harrison and Simons show that the bottom loss can be computed from an estimate $\hat{R}(\theta_b, \omega)$ of the power reflection coefficient obtained from array data as the ratio of the downward and upward beam powers:

$$\hat{R}(\theta_b, \omega) = \frac{\hat{B}(-\theta_b, \omega)}{\hat{B}(\theta_b, \omega)}. \quad (2)$$

BEAMFORMING BASIC EQUATIONS

Beamforming is a well-known spatial-filtering technique whose theory is treated in textbooks (e.g., [Johnson, 1993]); here we only report some equations that support previous and subsequent material. The *average beam power* $B(\phi, \omega)$ is defined as (for the sake of simplicity, in the following the dependence on frequency and grazing angle will often be dropped in the right-hand side of equations):

$$B(\phi, \omega) = E[\mathbf{w}^H \mathbf{p} (\mathbf{w}^H \mathbf{p})^H] = \mathbf{w}^H E[\mathbf{p} \mathbf{p}^H] \mathbf{w}. \quad (3)$$

In Eq.(3) H denotes the conjugate transpose operation, E denotes expectation and $\mathbf{w}(\phi, \omega) = [w_0, w_1, \dots, w_{M-1}]^T$ is the weight vector for the *steering angle* ϕ (T denotes the transpose operation). The angle $\phi = 0$ corresponds to the array being steered towards broadside (i.e., horizontally for a vertical array), $\phi > 0$ towards the surface, and $\phi < 0$

towards the bottom. The vector $\mathbf{p}(\omega) = [p_1(\omega), p_2(\omega), \dots, p_M(\omega)]^T$, where $p_m(\omega) = F \{p_m(t)\}$, represents the data from the M hydrophones in the array ($F \{ \cdot \}$ denotes the Fourier transform).

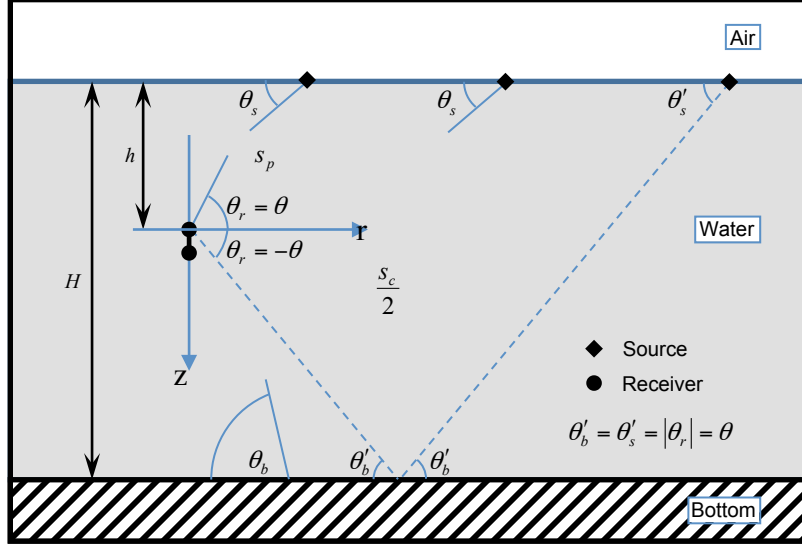


Figure 1: Definition of coordinate system and geometric quantities. For constant sound speed, the rays are straight lines (hatched), and $\theta'_s = \theta'_b = |\theta_r|$. The solid lines represent ray paths in the presence of a sound-speed profile. The same angle at the receiver θ_r is considered in both cases.

In real-world applications the spatial coherence matrix (or cross spectral density matrix, hereafter also referred to as “CSD matrix”) $\mathbf{C}_\omega = E[\mathbf{p}\mathbf{p}^H]$ is estimated by averaging the outer product over K snapshots:

$$\hat{\mathbf{C}}_\omega = \frac{1}{K} \sum_{i=1}^K \mathbf{p}_i \mathbf{p}_i^H. \quad (4)$$

and the average output power is then estimated as:

$$\hat{B}(\phi, \omega) = \mathbf{w}^H \hat{\mathbf{C}}_\omega \mathbf{w}. \quad (5)$$

Equation (2) shows that, in bottom-loss estimation, the ratio of the beamformer output power is used to estimate the power ratio of (plane) wave fronts incident upon the array from angles symmetric with respect to the horizontal.

BEAMFORMER ANGULAR RESOLUTION

Adopting the definition of resolution based on the Rayleigh criterion, and expressing the wave-propagation direction in terms of the vertical wavenumber, the angular resolution for a linear array is [Johnson, 1993]:

$$\Delta k = 2\pi/L, \quad (6)$$

where Δk is the distance between the two closest values of k that can be resolved and $L = d(M-1)$ is the total length of the array. Equation (6) shows that, for a given sensor spacing, increasing the number of array sensors (and therefore the array length) results in a finer resolution in k .

DERIVATION OF THE POWER REFLECTION COEFFICIENT FROM THE NOISE SPATIAL COHERENCE FUNCTION

The spatial coherence function of the pressure field $p(\mathbf{r}, t)$ between two points in space \mathbf{r}_1 and \mathbf{r}_2 is defined as the ensemble average of the product $p_\omega(\mathbf{r}_1)p_\omega^*(\mathbf{r}_2)$:

$$C_\omega(\mathbf{r}_1, \mathbf{r}_2) \equiv \langle p_\omega(\mathbf{r}_1)p_\omega^*(\mathbf{r}_2) \rangle, \quad (7)$$

where $*$ indicates complex conjugate and $p_\omega(\mathbf{r})$ is the coefficient of the Fourier expansion of $p(\mathbf{r}, t)$ at angular frequency ω . To make an explicit link to beamforming, element (i, j) in \mathbf{C}_ω is given by $C_\omega(\mathbf{r}_i, \mathbf{r}_j)$.

Using a ray-based approach Harrison derived a formula for the spatial coherence function of surface generated noise in the ocean, which for the case of two hydrophones joined by a perfectly vertical line and separated by a distance z is written [Harrison, 1996]:

$$C_\omega(z) = \int_0^{\pi/2} \frac{2\pi \sin \theta_s \cos \theta_r}{1 - R_s(\theta_s)R(\theta_b)e^{-as_c}} \cdot \left[e^{i(\omega/c)z \sin \theta_r} e^{-as_p} + R(\theta_b)e^{-i(\omega/c)z \sin \theta_r} e^{-a(s_c - s_p)} \right] d\theta_r. \quad (8)$$

In Eq.(8) θ_r , θ_s and θ_b are the ray angles at the receiver, the surface, and the bottom (see Figure 1); s_c and s_p are the complete and partial ray-path lengths; ω is the angular frequency; c is the sound speed at the receiver in the medium, and R and R_s are the bottom and surface power reflection coefficients. For the sake of simplicity, the dependence of the reflection coefficients on frequency will not be indicated explicitly. Note that a is the power attenuation per unit length. The model assumes that the hydrophones are “close”, so the ray paths and the sound speed are unambiguously defined. Now let:

$$k = \frac{\omega}{2\pi c} \sin \theta_r = \frac{\sin \theta_r}{\lambda}, \quad (9)$$

Where λ is the signal wavelength; then $0 < \theta_r = a \sin(\lambda k) < \pi/2$ gives the bounds $0 < k < 1/\lambda$. Note that Eq.(9) defines k as a scaled vertical wavenumber at the receiver: $k = k_z/2\pi$.

Eq.(8) is general enough to include the effects of volume absorption and a sound-speed profile in the water column. With some algebraic manipulation and moving Eq.(8) to the k domain by means of the Fourier transform, we were able to prove that $C_\omega(k)$, the k -spectrum of the coherence function, is split into a portion $\mathcal{F}^+(k)$, which is nonzero only for positive k values, and a portion $\mathcal{F}^-(k)$, which is nonzero only for negative k values, and that $R(k)$ can be computed as the ratio:

$$R(k) = \frac{\mathcal{F}^-(-k)}{\mathcal{F}^+(k)} e^{-a[2\tilde{s}_p(k) - \tilde{s}_c(k)]}, \quad k \in \left[0, \frac{1}{\lambda}\right]. \quad (10)$$

where the specific form of $\tilde{s}_c(k)$ and $\tilde{s}_p(k)$ depends on the sound-speed profile. Since negative values of k correspond to $\theta_r < 0$ and positive values of k correspond to $\theta_r > 0$ the result in Eq.(10) is reminiscent of the method for estimating R described by Harrison and Simons [Harrison, 2002]. They derived it through an energy-flux argument, whereas here a frequency-wavenumber domain derivation is presented.

SYNTHETIC-ARRAY PROCESSING

When working with array data, measurements are only available at the locations of the sensors, so the coherence function $C_\omega(z)$ is sampled at discrete intervals along the z axis, and the Fourier transform mentioned above must be interpreted as a discrete Fourier transform (DFT). As shown in Eq.(6), increasing the array aperture results in better resolution in the k domain. This results in increased angular resolution in the beamformer output, which translates into better estimation of the seabed bottom loss, but it comes at the price of physically increasing the array length. An alternative approach is synthetic-array processing, which is based on the idea of using measurements from a short array to approximate the CSD matrix of a longer array by exploiting the physical properties of $C_\omega(z)$. This section illustrates the procedure to obtain this “augmented” covariance matrix.

First, note that the dependence of $C_\omega(z)$ on the hydrophone-pair depth h appears implicitly in Eq. (8) in the difference between s_c and s_p ; its effect is quantified by the exponential correction factor in Eq.(10). The form of the exponential factor is such that at steep grazing angles the effect of sensor depth is minimal, while at shallow grazing

angles the correction factor is minimized by positioning the array close to the bottom. Furthermore, it has been theoretically proved and verified against experimental data for both deep [Liggett, 1966] [Barclay, 2013] and shallow water [Buckingham, 1980] [Harrison, 1996] that at sufficient distance from the waveguide boundaries, $C_\omega(z)$ depends mostly on the distance between the hydrophones, rather than their absolute position in the water column.

The spatial stationarity of $C_\omega(z)$ implies that equally-spaced hydrophones have the same coherence function, regardless of their position in the array. For the CSD matrix \mathbf{C}_ω , this means that, besides being *Hermitian* by construction, the matrix is *Toeplitz*. Synthetic-array processing exploits the *Hermitian-Toeplitz* structure of \mathbf{C}_ω to produce an approximation to the CSD Matrix of an array with a higher number of elements: For an M – element physical array, the positions on the $M - 1$ upper and lower diagonals of an “augmented” $2M \times 2M$ CSD matrix can be filled in accordance with the Hermitian-Toeplitz structure as shown in Figure 2.

In this study, as a first approximation, the remaining elements are filled with zeros, which is supported by the fact that the noise-only coherence function decays with increasing hydrophone spacing [Buckingham, 1980] [Harrison, 1996]. Therefore, if the number of elements in the array is sufficiently high, the error introduced by this approximation can be relatively small. However, it is still important to point out that the discontinuity in each row between the first or last nonzero element and the neighboring zero is not observed in real CSD matrices and can introduce artifacts in the estimation of the bottom loss, especially at low frequencies or for short arrays, as the wavelength becomes comparable to the array length (see Figure 3). To minimize these effects, it proved beneficial in this study to smooth the transition by applying an appropriate taper to the nonzero portion of each row.

$$\mathbf{C}_\omega = \begin{bmatrix} c_{1,1} & c_{1,2} & c_{1,3} \\ c_{1,2}^* & c_{2,2} & c_{2,3} \\ c_{1,3}^* & c_{2,3}^* & c_{3,3} \end{bmatrix} \xRightarrow{T} \begin{bmatrix} c_{1,1} & c_{1,2} & c_{1,3} & 0 & 0 & 0 \\ c_{1,2}^* & c_{1,1} & c_{1,2} & c_{1,3} & 0 & 0 \\ c_{1,3}^* & c_{1,2}^* & c_{1,1} & c_{1,2} & c_{1,3} & 0 \\ 0 & c_{1,3} & c_{1,2}^* & c_{1,1} & c_{1,2} & c_{1,3} \\ 0 & 0 & c_{1,3}^* & c_{1,2}^* & c_{1,1} & c_{1,2} \\ 0 & 0 & 0 & c_{1,3}^* & c_{1,2}^* & c_{1,1} \end{bmatrix}$$

Figure 2: CSD matrix “augmentation” for a 3-element array ($M = 3$). The augmentation step “ T ” is possible under the Toeplitz assumption and reduces significantly the number of arbitrary values in the augmented matrix.

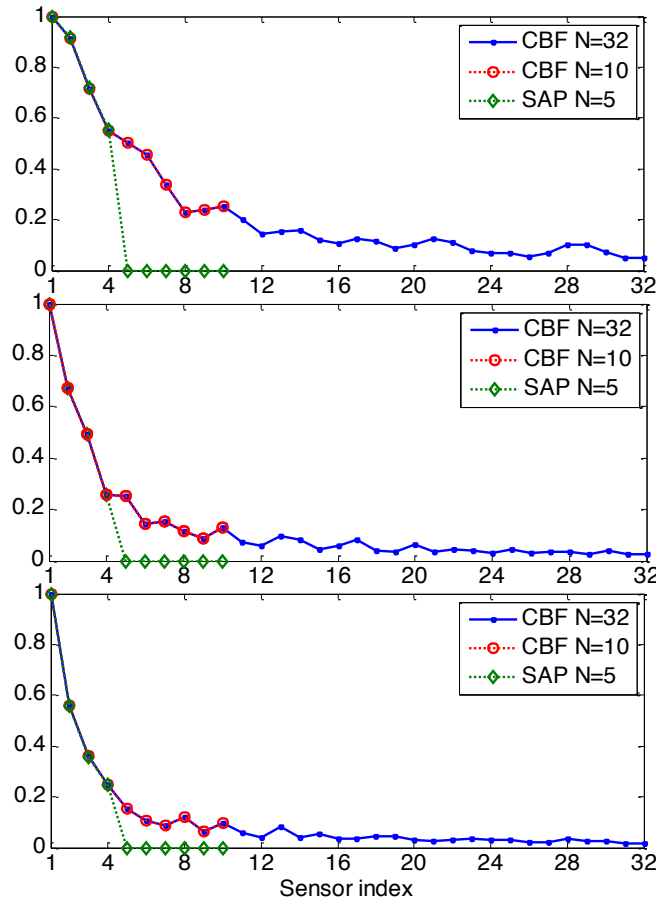


Figure 3: *Normalized magnitude of the first row of a cross spectral density matrix synthesized by OASN at 2020Hz (top), 4518Hz (center) and 5996Hz (bottom) for a conventional beamformer (CBF) with 32 and 10 physical sensors, and for a synthetic-array processor (SAP) with 5 physical sensors, extended to 10 sensors. The approximation introduced by the zeros becomes poorer at the lower frequencies.*

WORK COMPLETED

A new derivation in frequency-wavenumber domain of the reflection coefficient from the array spatial-coherence function has been developed, and synthetic-array processing has been formulated, tested in simulation and published [Publication #1]. The application of synthetic-array processing to measured experimental data has been presented at the 21st *International Congress on Acoustics* (June 2013, Montreal, Canada) [Publication #2].

RESULTS

BOTTOM-LOSS ESTIMATION FROM MEASURED DATA

The study included a preliminary phase [Publication #1] in which the synthetic-array processing was tested on CSD matrices produced by the OASN noise-simulation module of the OASES package [Schmidt, 2004], which implements a full wave solution based on wavenumber integration for horizontally stratified media. The bottom-loss estimates

shown in this section are obtained by processing array data acquired during three separate experiments by the NATO-STO Centre for Maritime Research and Experimentation (CMRE — formerly NATO Undersea Research Centre). The dataset identifiers used in this paper are reported in TABLE I, together with the basic features of the array.

TABLE I. Datasets and array basic features – all deployments were drifting, design frequency assumed at $c = 1500\text{m/s}$.

Dataset ID	Num. of elements	Spacing (m)	Sampling freq. (Hz)	Design freq. (Hz)
MFA-03	32	0.18	12000	4166
MFA-04	32	0.18	12000	4166
VLA-04	32	0.50	6000	1500

The CSD matrices are obtained from the Fourier transform of the acoustic data as indicated in Eq.(4), then used as $\hat{\mathbf{C}}_\omega$ in Eq.(5) to implement a conventional beamformer. The results from Eq.(5) are then used to compute \hat{R} as in Eq.(2), which is in turn substituted for R in Eq.(1), giving the bottom-loss estimate.

The bottom-loss profiles shown in Figure 4 refer to 5-minute averages from the MFA-03, MFA-04 and VLA-04 data, respectively. In all cases, analysis of the beam-power plots showed strong surface noise, noise notch and no discernible interferers. The two CBF curves correspond to profiles obtained using the full array (32 elements), and a shorter version composed of the first 16 elements. No ground truth is available for these data, so the estimate from the longer array is assumed to be the better one. The CBF curves show evidence of a marked degradation in angular resolution, in the case of the shorter array, in the form of less pronounced, wider peaks and valleys, and a generally lower loss estimated towards endfire, where the beams become wider. The SAP curves correspond to profiles obtained using only the first 16 elements of the array, but “augmenting” the CSD matrix to 32×32 elements by synthetic-array processing. The curves appear largely immune to the degradation experienced by the physical 16-element array, very closely resembling the performance of the 32-element physical array. Note that, given the larger inter-element spacing, the frequencies in the VLA-04 case are lower than in the others, but CBF and SAP compare in the same terms.

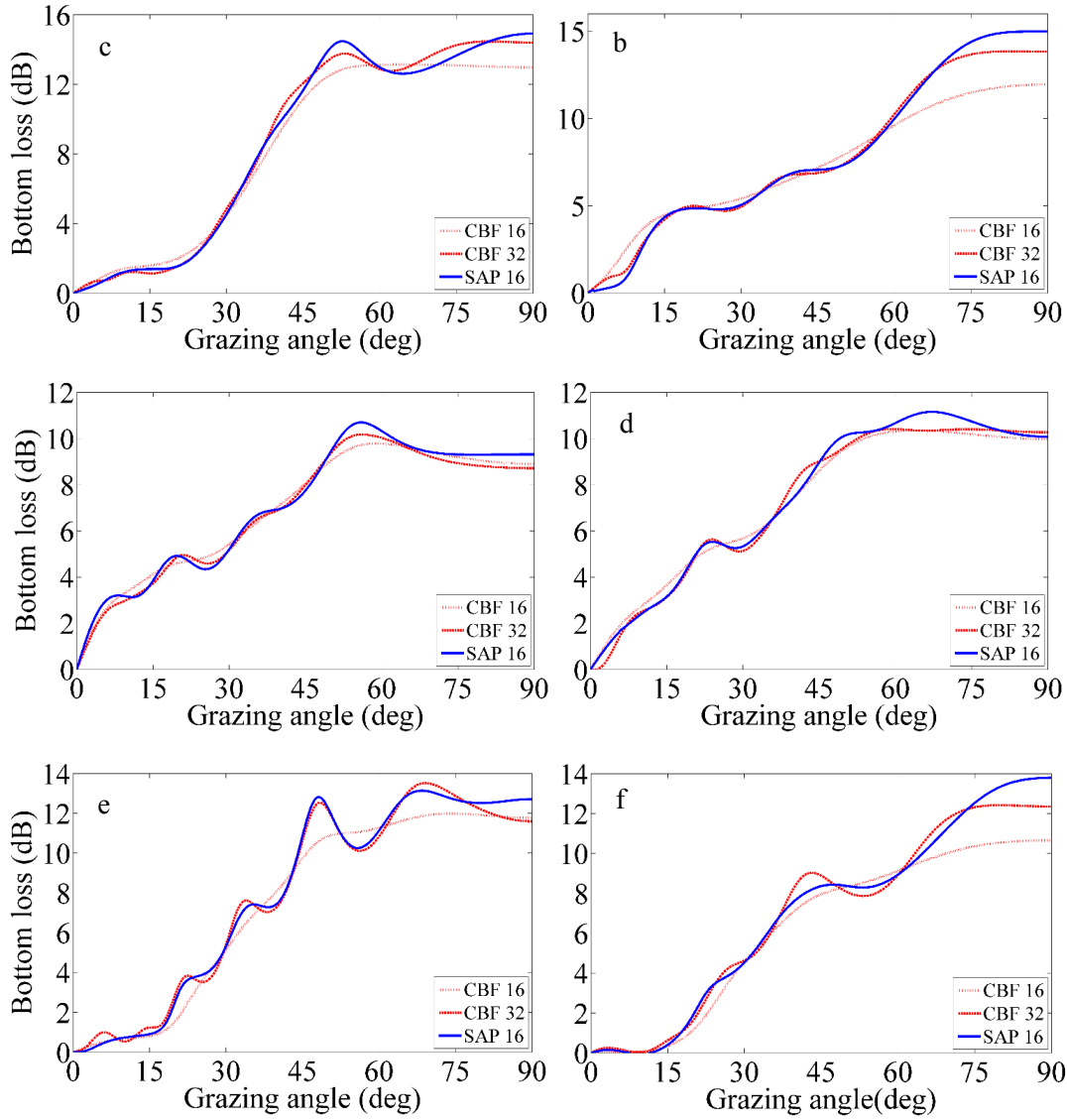


Figure 4: Bottom loss profiles computed from two 5-minute averages: MFA-03 data at 2766Hz (a) and 2250Hz (b), MFA-04 data at 3070Hz (c) and 3234Hz (d), and VLA-04 data at 1313Hz (e) and 972Hz (f): Conventional beamforming for 32-element and 16-element physical array vs. 16-element synthetic-array processor. The latter displays much reduced loss in angular resolution.

IMPACT/APPLICATIONS

This work may have a significant impact on several Navy sonar systems (e.g., ASW, MCM, underwater acoustic communications). Knowing the seabed properties will improve at-sea situational awareness by being able to accurately predict acoustic propagation. And, because this is a passive method it can be designed into a system used for covert activities, low power applications and can be used even in environmentally restricted areas.

REFERENCES

- [Harrison, 2002] C. H. Harrison and D. G. Simons, "Geoacoustic inversion of ambient noise: A simple method," J. Acoust. Soc. Am., **112**, 1377-1389 (2002).
- [Harrison, 1996] C. H. Harrison, "Formulas for ambient noise level and coherence," J. Acoust. Soc. Am. **99**, 2055-2066 (1996).
- [Johnson, 1993] D. H. Johnson and D. E. Dudgeon, *Array signal processing concepts and techniques*, (Prentice-Hall, Upper Saddle River, 1993).
- [Liggett, 1966] W. S. Liggett and M. J. Jacobson, "Noise covariance and vertical directivity in a deep ocean," J. Acoust. Soc. Am. **39**, 280-288 (1966).
- [Barclay, 2013] D. R. Barclay and M. J. Buckingham, "Depth dependence of wind-driven, broadband ambient noise in the Philippine Sea," J. Acoust. Soc. Am. **133** 62-71 (2013).
- [Buckingham, 1980] M. J. Buckingham, "A theoretical model of ambient noise in a low-loss, shallow water channel," J. Acoust. Soc. Am. **67**, 1186-1192 (1980).
- [Schmidt, 2004] H. Schmidt, OASES Version 3.1 User Guide and Reference Manual, Massachusetts Institute of Technology, <http://acoustics.mit.edu/faculty/henrik/oases.html>, Cambridge, MA, (2004).

PUBLICATIONS

1. M. Siderius, L. Muzi, C. H. Harrison, and P. L. Nielsen, "Synthetic array processing of ocean ambient noise for higher resolution seabed bottom loss estimation," J. Acoust. Soc. Am., **133**, EL149-EL155 (2013). [Accepted, refereed]
2. L. Muzi and M. Siderius, "Synthetic-array beamforming for bottom-loss estimation using marine ambient noise," J. Acoust. Soc. Am., Proceedings on Meetings in Acoustics (POMA) **19**, 070033 (2013). [Conference]

HONORS/AWARDS/PRIZES

Publication #2 won first place in the Best Student-Paper Award for Underwater Acoustics at the 21st International Congress on Acoustics (June 2013, Montreal, Canada).